Geophysical Research Letters

RESEARCH LETTER

10.1029/2023GL103351

Distinctly Different Dynamical Processes in Maintaining the Intraseasonal NAO+ and NAO−

Jiwang Ma[1,2] and **X. San Liang**[1,2,3]

[1]Department of Atmospheric and Oceanic Sciences, Fudan University, Shanghai, China, [2]The Artificial Intelligence Group, Division of Frontier Research, Southern Marine Laboratory, Zhuhai, China, [3]IRDR ICoE on Risk Interconnectivity and Governance on Weather/Climate Extremes Impact and Public Health, Fudan University, Shanghai, China

Key Points:

- The well studied eddy forcing to the intraseasonal NAO is actually only limited to its negative phase
- In the positive phase NAO+, the lack of eddy forcing is compensated by a strong barotropic instability at the center
- Both the basic flow-NAO interaction and the eddy-NAO interaction are asymmetric in phase

Supporting Information:

Supporting Information may be found in the online version of this article.

Correspondence to:

X. S. Liang,
xsliang@fudan.edu.cn

Citation:

Ma, J., & Liang, X. S. (2023). Distinctly different dynamical processes in maintaining the intraseasonal NAO+ and NAO−. *Geophysical Research Letters*, *50*, e2023GL103351. https://doi.org/10.1029/2023GL103351

Received 18 FEB 2023
Accepted 29 APR 2023

Abstract Positive feedback between high-frequency eddies and low-frequency processes is believed to play an essential role in the NAO evolution. In this study, however, it is found that the previously well-studied upscale forcing to the intraseasonal scale window is mostly limited during the phase NAO−, but almost disappears during NAO+. The maintenance of the intraseasonal NAO+ is by a strong barotropic instability of the basic flow, which has been overlooked previously. The divergence of the Reynolds stress tensor that decelerates the basic flow is found to account for this asymmetry. For NAO−, there also exist strong interactions between the basic flow and the intraseasonal component, but the energy transfer is in a dipolar form, which, if integrated over space, contributes insignificantly as a whole. These new findings from a dynamics viewpoint shed insight deeper into NAO, a climate mode playing a key role in the Northern Hemisphere warming.

Plain Language Summary Understanding the dynamics of NAO is of both scientific and societal importance because of its role in global warming. Traditionally it is well recognized that NAO is mainly forced by the stormy synoptic eddies via upscale forcing. This study demonstrates that, using a state-of-the-art multiscale analysis methodology, that the upscale eddy forcing to the low-frequency processes only plays its role in a particular phase, that is, the negative phase, if what we focus is the intraseasonal NAO component. In the positive phase the energy source is mainly from a strong barotropic instability of the basic flow in the center of the NAO dipole. These findings are expected to help construct more reliable models for a more accurate prediction of NAO.

1. Introduction

North Atlantic Oscillation (NAO) is one of the dominant low-frequency mode over the North Hemisphere. It has two phases—positive and negative phases, written respectively as NAO+ and NAO−. During the positive (negative) phase, it consists of an Ice Island low (high) and Azores high (low) (Hurrell et al., 2003; Walker & Bliss, 1932). A substantial proportion of the Northern Hemisphere warming can be projected onto NAO (Cohen & Barlow, 2005; Hurrell, 1995, 1996). Understanding its dynamics is hence critical in order to better comprehend and foresee the climate change on our planet.

A fact is that NAO has footprints on different components of low-frequency processes, from intraseasonal to interannual scales (Barnston & Livezey, 1987; S. B. Feldstein, 2000; Rennert & Wallace, 2009). From a synoptic point of view, it has an intraseasonal e-folding time of approximately 2 weeks (S. B. Feldstein, 2000). Ren et al. (2022) find an intraseasonal evolution of interactions between the high-frequency and low-frequency processes in a two-scale framework by projecting the eddy-vorticity forcing to the 20–60-day-filtered NAO index. Rennert and Wallace (2009) find that the NAO development is accompanied by an enhancement of intraseasonal waves. More importantly, NAO might be the source of predictability for the extending weather forecast beyond the current limit, since its precursors can be found in the stratosphere from weeks up to 2 months ahead of time (Baldwin & Dunkerton, 1999, 2001; Thompson & Wallace, 1998), which is also in the intraseasonal frequency band. The above facts tell that the intraseasonal variabilities of NAO is essential to its evolution.

Lying at the heart of the extratropical low-frequency dynamics are the interactions between the low-frequency processes and synoptic eddies. In particular, a positive feedback is regarded essential in many studies (Barnes et al., 2010; Barnes & Hartmann, 2010; Cai & Mak, 1990; S. Feldstein & Lee, 1998; Jin et al., 2006; Jin, 2009; Kug & Jin, 2009; Limpasuvan & Hartmann, 1999; D. J. Lorenz & Hartmann, 2001; Luo et al., 2007, 2015; Ren et al., 2009, 2012; Robinson, 1991, 1996, 2000, 2006; Song, 2016; Zhang et al., 2012). However, as mentioned above, the low-frequency processes possess a range of components and how the synoptic storms interact with these components, including intraseasonal processes which is of great importance in understanding the NAO dynamics, is not clear. Furthermore, Rennert and Wallace (2009) find significant cross-frequency coupling between low-frequency and intermediate processes during NAO, which infers interaction between low-frequency and intraseasonal processes. We are hence investigating the interactions between the high-frequency processes and the intraseasonal components of the low-frequency NAO through separating all the variables into three scales, namely, basic flow scale, intraseasonal scale and high-frequency scale, and then diagnose the kinetic energy cascades among these scales. In such a three-scale framework, we can also address an issue overlooked in previous NAO studies—the interaction between the intraseasonal processes and basic flow.

2. Data and Methods

2.1. Data

The NAO index is obtained from the Climate Prediction Center of National Oceanic and Atmospheric Administration (Barnston & Livezey, 1987). We use the ERA-40 (https://apps.ecmwf.int/datasets/data/era40-daily/levtype=pl/) data set from the European Centre for Medium-Range Weather Forecasts (ECMWF) (Uppala et al., 2005), including temperature (T), wind velocity (u, v, ω), geopotential (Φ), among other fields, with a time resolution of 6 hr and a spatial resolution of 2.5° × 2.5°. Horizontally it covers the zonal circle between 30° and 85°N, and vertically it has 15 standard p levels, ranging from 1,000 to 50 hPa. We choose a period with 2^{16} time steps, starting 1 September 1957, and ending 21 May 2002. This is because the analysis methodology (see below) requires that the time steps be arranged to be a power of 2.

2.2. Multiscale Window Transform, Multiscale Energetics Analysis, and Canonical Transfer

2.2.1. Multiscale Window Transform

In 2007, Liang and Anderson developed a functional analysis apparatus, namely, multiscale window transform (MWT), for multiscale energetics studies (Liang & Anderson, 2007). While orthogonally decomposing a field by scale, in order to provide filtered fields (reconstructions), MWT also provides transform coefficients, just like the transform coefficients in Fourier space, for the corresponding filtered fields, which are lacked in the widely used localized traditional filters such as the Butterworth filter. This ensures energy conservation during a decomposition (thanks to the Parseval relation in functional analysis), and, besides, makes it possible to express multiscale energies in terms of the resulting transform coefficients. This is in contrast to most of the widely used filters, which do not have transform coefficients and hence actually cannot have this multiscale energy representation. Recall that, in the literature, it is a common practice to use the square of a filtered field as the multiscale energy of that field. This is, unfortunately, conceptually wrong—just think about the energy in Fourier space when examining a power spectrum.

With MWT a field can be reconstructed onto some range of scales, or *scale windows* as called. In this study we will need a basic flow window, an intraseasonal scale window where lies the NAO signal (or simply NAO window if no confusion may arise in the context), and a high-frequency window. For convenience, we will denote these windows as 0, 1, 2, respectively. A more comprehensive introduction of MWT is beyond the scope of this study; interested readers are referred to Liang and Anderson (2007) for details, or to Liang (2016) for a more readable short introduction. Here we simply write the MWT of a field, say T, as $\hat{T}_n^{\sim\varpi}$, where n is the time step, $\varpi = 0, 1, 2$ denotes the scale window. The corresponding reconstructions, that is, filtered fields, are written as $T_n^{\sim\varpi}$. More details are referred to the Supporting Information S1, where a brief introduction of MWT is supplied.

2.2.2. Canonical Transfer

Multiscale energetics analysis has become a powerful tool to diagnose the dynamical processes underlying atmospheric phenomena, thanks to E. N. Lorenz (1955)'s seminal work. Lorenz's formalism, however, is in an integral/average form, lacking the needed local information for most of the weather and climate processes. In the literature, there are many studies attempting to get around this difficulty by simply removing the average operators. This simple practice seems to be effective, but, unfortunately, is conceptually incorrect. As elaborated in Liang (2016) and many other publications, a most recent one being Yang et al. (2020), that removing the average operator from the eddy energy formula with a Reynolds decomposition does not yield the "localized eddy energy"; in fact, it is not at all energy in the physical sense. The average operator allows for a connection of the so-obtained eddy energy to the eddy energy in the Fourier space through the renowned Parseval identity in functional analysis; otherwise the so-obtained "energy" would not be conserved. Second, localizing the bulk Lorenz formalism is faced with an obstacle on how to separate the cross-scale transfer from in-scale transport, which is rather subjective in classical formalisms and not unique. This is a rather fundamental problem (as identified in some early pioneering studies such as Plumb, 1983) which, however, has been mostly overlooked. Liang and Robinson (2005, 2007) is the first to tackle this systematically, using the aforementioned MWT as the machinery. The thus-obtained transfer is proved to be unique later on by Liang (2016), and bears a Lie bracket form (just like the Poisson bracket in Hamiltonian dynamics), satisfying the Jacobian identity, among many other properties. Accordingly, it has been termed as *canonical transfer*. In the following we simply write out the formula for computation; the reader is referred to Liang (2016) for details.

As proved in Liang (2016), for a scalar field T in an incompressible flow $\boldsymbol{v}$, the canonical transfer to scale window ϖ from all other scale windows at time step n is

$$\Gamma_n^{\varpi} = -\mathrm{E}_n^{\varpi} \nabla \cdot \left[\frac{\widehat{(\mathbf{v}T)}_n^{\sim\varpi}}{\widehat{T}_n^{\sim\varpi}} \right], if\ \widehat{T}_n^{\sim\varpi} \neq 0, \tag{1}$$

where $\mathrm{E}_n^{\varpi} = \frac{1}{2}\left(\hat{T}_n^{\sim\varpi}\right)^2$ is the multiscale energy on window ϖ at time step n. This transfer has a nice property $\sum_{\varpi}\sum_{n}\Gamma_n^{\varpi} = 0$, which means that this kind of process only redistributes energy among scales; it does not generate nor destroy energy as a whole; in other words, it ensures energy conservation, in contrast to the traditional counterparts. It has been established that, in the most particular case, that is, the case with the Reynolds decomposition, (Equation 1) integrated over the whole spatial domain is precisely the traditional Lorenz formalism (Liang & Robinson, 2007). So it can be viewed as a local extension of the Lorenz formalism.

MWT and the MWT-based multiscale energetics analysis have been validated with benchmark geophysical fluid dynamical processes (e.g., Liang & Robinson, 2007), and applied with success in many real atmosphere-ocean-climate problems. The most recent ones include those on storm track (Y.-B. Zhao et al., 2019), atmospheric blocking (Ma & Liang, 2017), cold wave outbreak (Xu & Liang, 2020), Gulf of Mexico circulation (Yang et al., 2020), to name but a few.

3. Results

Using MWT as a filter, the original fields are separated into three scale windows, that is, the basic flow window (above 64 days), intraseasonal window (16–64 days) and high-frequency window (less than 16 days). The canonical kinetic energy (KE) transfers from the basic flow window and the high-frequency window to the intraseasonal window are evaluated by Equation 1. Then the required resulting variables for analysis are composited with respect to the NAO+ and NAO− instants, which correspond to the NAO index larger than its standard error, δ, and that less than $-\delta$, respectively. The composite intraseasonal component and the KE transfers between it and other two scale windows are shown below. Since the basic flow varies significantly with season, only the NAO instants in winter are composited. It should be pointed out that November and March are also included into the "winter" here to incorporate more NAO events to ensure statistical significance for the composition; that is to say, "winter" is used to represent November through March hereafter. Frequently one may see that some processes on the NAO scale window and the corresponding climatological ones are similar. As pointed out by Hansen and Sutera (1984) and Kushnir (1987), among others, these processes can not be used to explain the development of NAO. For this reason, we will only analyze the canonical KE transfer differences from the winter climatology. For reference convenience, we will still refer to these differences as KE transfers; that is to say, from now on, the canonical transfers should be understood as the canonical transfers with their respective climatologies removed.

3.1. Asymmetry Between the Intraseasonal Components of NAO+ and NAO−

Asymmetry in strength between NAO+ and NAO− has been identified in previous studies (Barnes & Hartmann, 2010; Luo et al., 2018). Notice that, in those studies, the NAO signal includes both the basic flow and intraseasonal components which here we will distinguish. Taking advantage of the three-window framework,

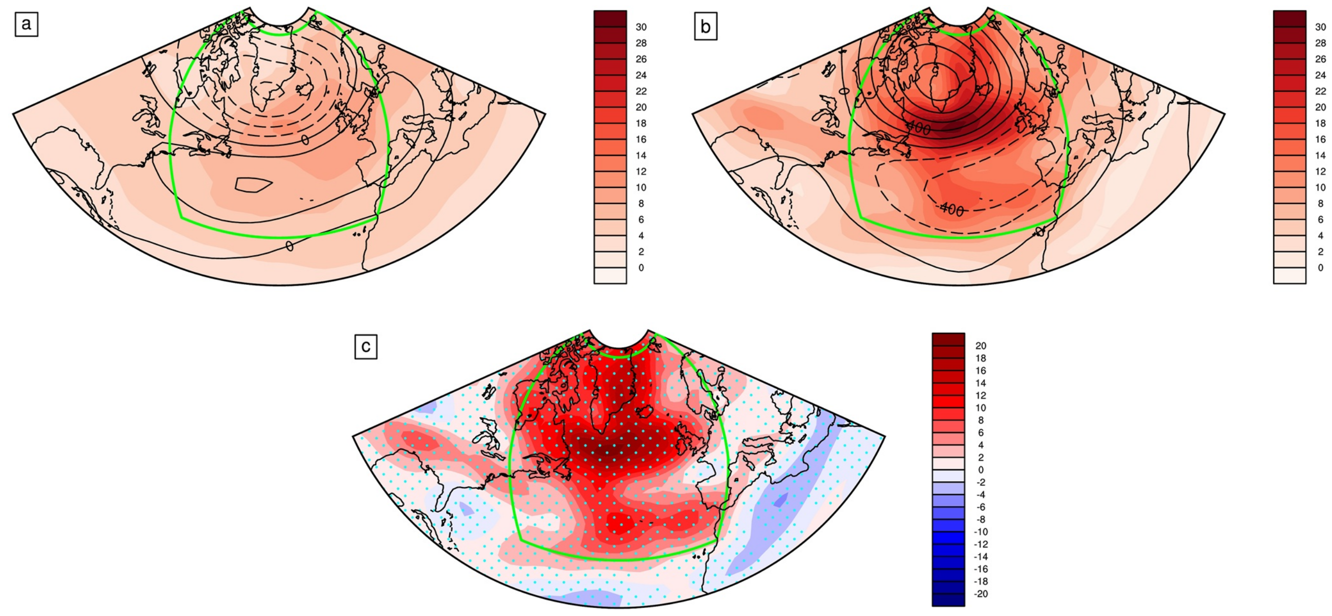

Figure 1. Composite geopotential (at 250 hPa, contoured, in m^2/s^2) and KE (averaged from 1,000 hPa through 200 hPa, shaded, in m^2/s^2) on the intraseasonal window during (a) NAO+ and (b) NAO−, and (c) difference between the KE fields during NAO− and NAO+. Dotted are the regions of KE statistically significant at the 99% level by the Student's *t* test. Green box circles the critical region of NAO dynamics where in Figure 3 are averaged.

here we are able to single out the intraseasonal component, and hence investigate the corresponding asymmetry. A recent study also emphasizes the asymmetry in dependence of NAO+ and NAO− on their precursors (Schmith et al., 2022), implying dynamical difference between NAO+ and NAO−. Shown in Figure 1 are the intraseasonal geopotential and KE for NAO+ and NAO−. As can be seen, both the geopotential and KE during NAO− (right panel) is stronger than their counterparts during NAO+ (left panel). For NAO− (right), the maximum geopotential magnitudes on the intraseasonal window reach 1,000 m^2/s^2 in the northern high cell, while it is only 800 m^2/s^2, for NAO+ (left). Similarly, the maximum KE is evidently stronger during NAO− than during NAO+. By checking the difference between the intraseasonal KE fields during NAO− and NAO+, we find that they are most significantly different at the transition zone of the two NAO cells over south of Greenland.

3.2. Upscale Transfer From the High-Frequency Window

Upscale transfer of energy is ubiquitous over the extratropical region. Its critical role is recognized in the maintenance of low-frequency processes, such as the jet stream (e.g., Oort, 1964), teleconnections (e.g., S. Feldstein & Lee, 1998; D. J. Lorenz & Hartmann, 2001; Robinson, 2000), and blocking (e.g., Green, 1970; Luo, 2005; Ma & Liang, 2017; Shutts, 1983), etc. Usually the low-frequency processes are almost regarded as a bulk in most of the previous studies; as a result, it is difficult to related the upscale transfer accurately to one of the components of the low-frequency processes. Here, by taking advantage of the three-scale window decomposition, a somewhat surprising finding is that upscale transfer is not always dominant in the development and maintenance of the intraseasonal low-frequency process; it depends on their phases (Figures 2a and 2b). This is demonstrated by the significant contrast of the upscale transfer during NAO− and NAO+. During NAO−, a substantial part of the upscale transfer occupies the NAO region. In contrast, during NAO+ the interactions between the high-frequency window and the intraseasonal window are much weaker, and the intraseasonal window even loses KE to the high-frequency window at the center of the low cell. This observation demonstrates that the upscale transfer to the low-frequency processes, which is well-recognized in previous studies, only dominates in particular phase if only the intraseasonal NAO component is focused on.

The difference between the upscale transfers during NAO+ and NAO− accounts for the asymmetry in intraseasonal KE as mentioned above. A stronger upscale transfer during NAO− leads to a stronger intraseasonal process during NAO−, and vice versa. This is consistent with Barnes and Hartmann (2010), though what they investigate are all the low-frequency component, not only the intraseasonal component here. The new finding here is that upscale transfer is nearly absent in NAO+ when only the intraseasonal component is considered.

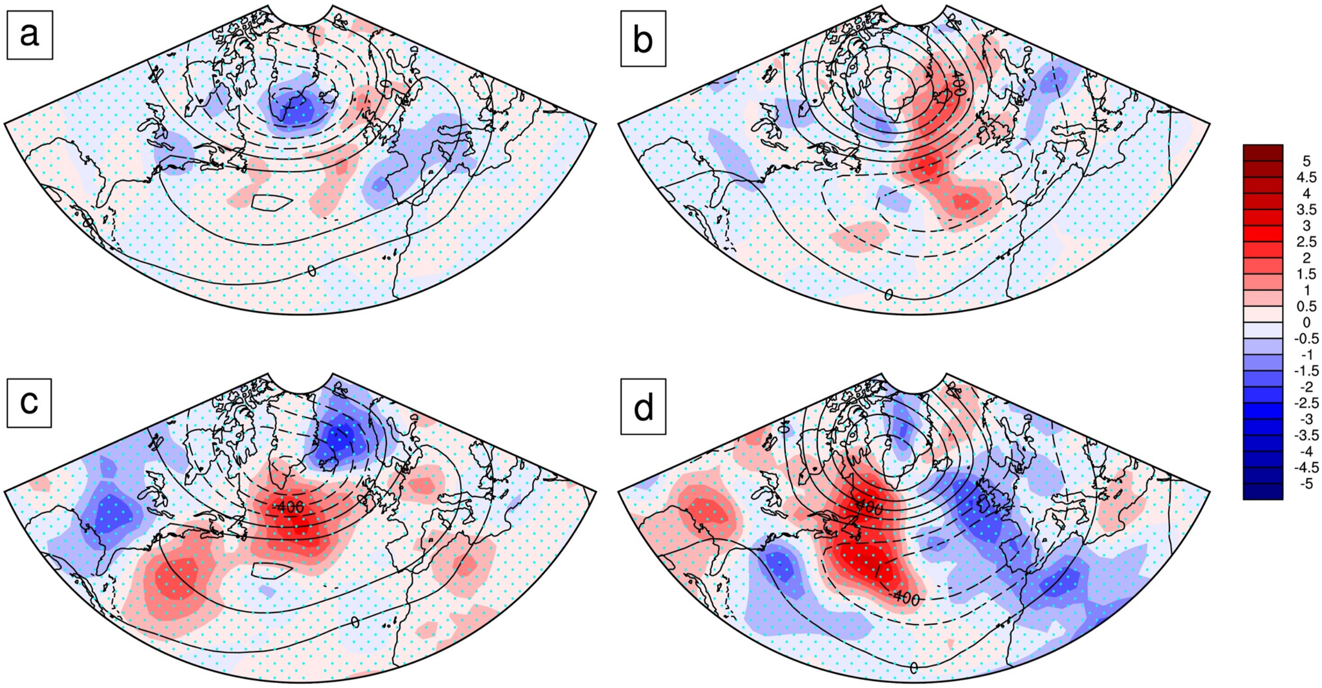

Figure 2. Composite geopotential (at 250 hPa, contoured, in m^2/s^2), canonical KE transfer from the high-frequency window to the intraseasonal window ($\Gamma_K^{2\to1}$, averaged from 1000 hPa through 200 hPa, shaded, in $10^{-4}m^2/s^3$) during (a) NAO+ and (b) NAO−, canonical KE transfer $\Gamma_K^{2\to1}$ from the basic flow to the intraseasonal window ($\Gamma_K^{0\to1}$, averaged from 1,000 hPa through 200 hPa, shaded, in $10^{-4}m^2/s^3$) during (c) NAO+ and (d) NAO−. Dotted are the regions of $\Gamma_K^{2\to1}$ and $\Gamma_K^{0\to1}$ statistically significant at the 99% level by the Student's *t* test.

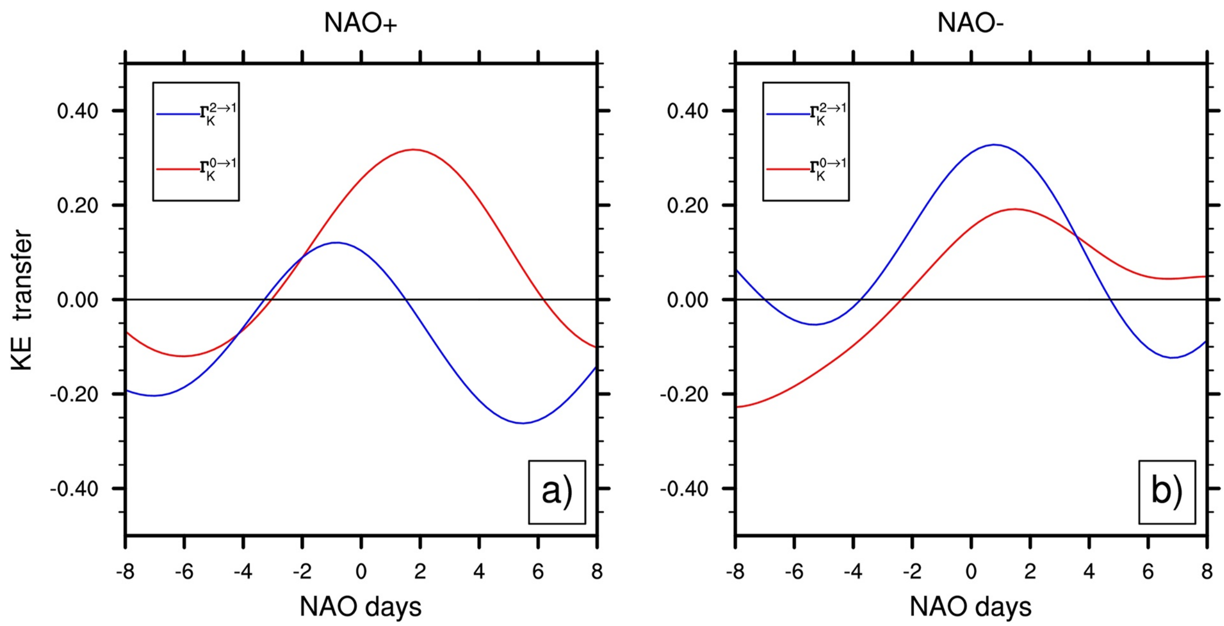

Figure 3. Time series of the KE transfer from the basic flow window (red lines, $\Gamma_K^{0\to1}$, in $10^{-4}m^2/s^3$) and that from the high-frequency window (blue lines, $\Gamma_K^{2\to1}$, in $10^{-4}m^2/s^3$) to the intraseasonal window for (a) NAO+ and (b) NAO−, respectively. The KE transfers are averaged from 1,000 hPa through 200 hPa over the region marked by the green box in Figure 1. The black line in the middle is the abscissa.

3.3. Barotropic Instability

Quite different from the well-recognized upscale forcing of high-frequency eddies, the role of barotropic instability of the basic flow has attracted much less attention in the low-frequency NAO dynamical studies. Here in the three-window framework, one can easily investigate this by examining the canonical KE transfer from the basic flow window to the intraseasonal window ($\Gamma_K^{0\to1}$).

For NAO+, we can find three significant features from the pattern of $\Gamma_K^{0\to1}$ (Figures 2c and 2d). Within the northern cell at relatively high latitudes is a dipole, with a positive patch in relatively small magnitude in the west and a strong negative patch in the east. Within the southern cell is a strong zonal dipole of $\Gamma_K^{0\to1}$ (a negative center over Gulf of Mexico and US, plus a positive center to its east). In between the southern and northern cells is a transition zone, where lies a strong positive $\Gamma_K^{0\to1}$. For NAO−, by checking the same northern and southern cell regions as above, we find that generally the $\Gamma_K^{0\to1}$ features are similar, except for a minus sign (a reflection of the opposite phase). However, in the transition zone between the cells, the distributions are completely different. While during NAO+ sandwiched between the cells is a strong positive center of $\Gamma_K^{0\to1}$ over the Atlantic, during NAO− the same region is replaced by a dipole, with a positive center in the west and a negative one in the east.

These above observations tell that the dynamics of NAO+ and NAO− are nearly antisymmetric, except for the transition zone, where the two are very different. For NAO−, it is a dipole with a positive center at the west and a negative one at the east; while for NAO+, there is only a positive center. Recalling the intraseasonal KE distribution in Figure 1, one can easily find that the transition zone is where the intraseasonal scale window KE concentrates. In this sense, it is a rather critical region for NAO dynamics. If we evaluate the role of $\Gamma_K^{0\to1}$ at the transition zone in a bulk view, it is then clear that the canonical KE transfer from the basic flow to the intraseasonal window contributes significantly to the NAO+ development, but does not make a significant contribution for the NAO− development since the positive and negative parts of the $\Gamma_K^{0\to1}$ dipole almost cancel out. The new finding here is that, during NAO+, the positive contribution from the basic flow to the intraseasonal window compensate the relatively weak upscale transfer from the eddy forcing (cf. Figures 2a and 2b). In other words, it is the barotropic instability of the basic flow that contributes majority to the development and maintenance of NAO+, while eddy forcing makes the major contribution to NAO−. These new findings provide evidence for the theoretical studies of DeWeaver and Nigam (2000a, 2000b) and Kimoto et al. (2001), who propose that the interaction between the mean-flow and stationary waves can be essential to the NAO-like mode.

Recall that the KE (or strength) of NAO− is significantly larger than that of NAO+ (cf. Figure 1). To examine the possible contributions of the KE transfers in causing this asymmetry, the KE transfer from the high-frequency window and the basic flow window to the intraseasonal window are integrated over the region where the KE of NAO concentrates, as circled by the green box in Figure 1. For NAO+, values of the former and the latter are −0.004 and 0.12 $\mathrm{m}^2/\mathrm{s}^3$. While for NAO−, they are 0.14 and 0.07 $\mathrm{m}^2/\mathrm{s}^3$. Summation of these two processes for NAO+ and NAO− are 0.116 and 0.21 $\mathrm{m}^2/\mathrm{s}^3$, respectively. Clearly, the difference of KE transfers from the basic flow and the high-frequency window to the intraseasonal window can partially account for the asymmetry in NAO magnitude at different phases, and their ratio is nearly 116:210.

3.4. Time Evolution of Barotropic Instability and Upscale Eddy Forcing

To further elucidate the role of the above two processes, that is, barotropic instability and upscale KE transfer, in the evolution of NAO+ and NAO−, their temporal evolution is plotted with respect to NAO lifecycle. The green box in Figure 1 marks the region where the KE and KE difference signals of NAO+ and NAO− are concentrated. In other words, this region is critical in controlling NAO dynamics. We hence averaged barotropic instability and upscale KE transfer over this region. NAO+ and NAO− events are first selected before the composition. If the NAO index is greater than its standard error, δ, for at least successive 5 days, the event is defined as an NAO+ event. Similarly, that with the index less than $-\delta$ for at least successive 5 days is defined as an NAO− event. In such a manner, 102 and 78 NAO+ and NAO− events in winter are selected. For each event, the day when its strength attains maximum is defined as NAO day 0, the day before and after that is subsequently defined as day …−3, −2, −1 and day 1, 2, 3…, respectively. The barotropic instability and upscale KE transfer from the high-frequency window to the intraseasonal window on the same NAO day are then composited, with the results shown in Figure 3. Generally speaking, barotropic instability is much larger (less) than upscale transfer/eddy forcing during NAO+ (NAO−) events. This is consistent with the above analysis. Further check on them on different

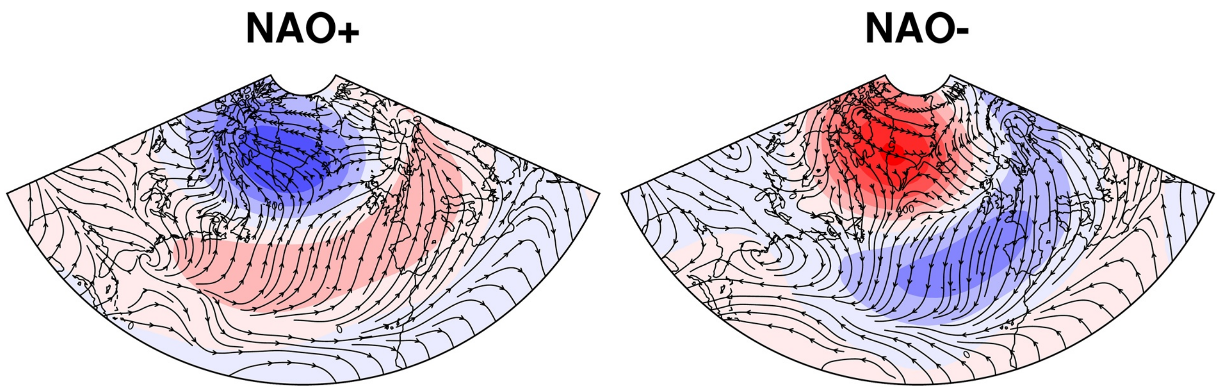

Figure 4. Streamlines of $\overline{\mathbf{v}'u'}$. The left (right) is for NAO+ (NAO−). The shaded is the geopotential on the intraseasonal window, which is used to denote the NAO location.

stages of NAO tells us that the upscale eddy forcing attains its maximum when NAO is strongest near day 0 for both NAO+ and NAO−, while barotropic instability is maximized after the strongest days of NAO+ and NAO− events. By this observation, these KE transfers are pivotal in maintaining NAO.

4. Discussion

It would be of interest to understand the dynamics deep in the cross-scale interactions. For clarity, we consider an idealized configuration, which is very close to the realistic configurations of the transition zone between the two cells of NAO+ and NAO−. We further simplify the problem by considering it within the Reynold decomposition framework, that is, to represent the high-frequency processes and the NAO signals as, respectively, perturbations and time-means, so that the total flow u can be decomposed as $\overline{\mathrm{u}} + \mathrm{u}'$. For an idealized basic flow profile ($\overline{\mathrm{u}}$ (y),0), the canonical KE transfer between the NAO and high-frequency processes is reduced to (Liang & Robinson, 2007)

$$(1/2)\left[\overline{u}\nabla\cdot\overline{(\mathbf{v}'u')} - \overline{(u'v')}\partial\overline{u}/\partial y\right] \tag{2}$$

Albeit idealized, the basic flow is very close to the real flow between the two cells of NAO+ and NAO− (cf. the contours in Figure 2). We calculate the two terms in (Equation 2) respectively and find that the first term dominates in the transition zone.

A closer look at the first term, that is, $\overline{u}\nabla\cdot\overline{(\mathbf{v}'u')}$, reveals that it is a product of the background velocity and the divergence of the *negative* Reynolds stress [recall $\overline{-(\mathbf{v}'\mathrm{u}')}$ is the Reynolds stress tensor) in the direction of u'. Recall that, by fluid dynamics theory, the divergence of a stress tensor means a force. To illustrate, suppose we have a stress tensor $\mathbf{T}$, and want to find its corresponding flow field $\mathbf{v}$. For simplicity, neglect gravity and rotation, and take the density of the fluid as a constant (hence incompressible). Now consider an arbitrary volume V, and denote its boundary (a surface) as S. Then by Newton's second law, $\frac{d}{dt}\iiint_V \mathbf{v}d\mathrm{V} = \iint_S \mathbf{T}\cdot\mathbf{n}d\sigma$. By Reynolds' transport theorem, the left hand side is $\iiint_V\left(\frac{\partial \mathrm{v}}{\partial t} + \nabla\cdot(\mathbf{vv})\right)d\mathrm{V}$, which is $\iiint_V\left(\frac{\partial \mathrm{v}}{\partial t} + \mathbf{v}\cdot\nabla\mathbf{v}\right)d\mathrm{V}$ due to the incompressibility. By Gauss' theorem, the right hand side is $\iiint_V \nabla\cdot\mathbf{T}dV$. Since V is arbitrary, we have

$$\frac{\partial\mathbf{v}}{\partial t} + \mathbf{v}\cdot\nabla\mathbf{v} = \nabla\cdot\mathbf{T}$$

So the divergence of a stress tensor will drive a flow $\mathbf{v}$ = (u,v,w). As $\mathbf{T} = \overline{-(\mathbf{v}'\mathbf{v}')}$ is the Reynolds stress tensor, its divergence must drive a secondary flow modifying the basic field.

By this argument, here $\nabla\cdot\overline{(\mathbf{v}'u')}$ means the eddy force due to the Reynolds stress that decelerates $\overline{u}$, so the product of it with $\overline{u}$, $\overline{u}\nabla\cdot\overline{(\mathbf{v}'u')}$, means the work done by the eddy force in decelerating the basic flow. In other words, a divergent region of $\overline{(\mathbf{v}'u')}$ is where the basic flow is decelerated by the eddy forcing (increasing easterlies or decreasing westerlies). Figure 4 shows the divergence of $(\overline{\mathbf{v}'u'})$. It is clear that there are significant divergent flows in the transition zone of NAO− but not for NAO+. This means that *eddies exert a forcing to NAO− but not to NAO+ in the transition zone.* The decelerating role of the eddies further demonstrates that it helps the development of easterlies in the transition zone of NAO−. From the aspect of energy transfer, this means an upscale transfer of energy. As we know, NAO− is accompanied by decelerating zonal winds while NAO+ by accelerating zonal winds. By the above argument, the eddy forcing does not work for NAO+. The finding in this study that eddies only forces NAO− is hence physically reasonable.

5. Conclusions

We have investigated the role of multiscale interaction on the intraseasonal component of NAO and its evolution in a three-scale window framework, using the multiscale window transform (MWT) and the theory of canonical transfer, as rigorously developed earlier on (cf. Liang, 2016). First, the field variables are decomposed into three scale windows, that is, the basic flow window (above 64 days), intraseasonal window (16–64 days) and high-frequency window (less than 16 days). This decomposition allows us to study in a systematic way the interactions between the intraseasonal component of the low-frequency process and the high-frequency storms, and between that and the basic flow, distinguishing this study from others in which all the low-frequency processes are treated in a bulk form, and the role of basic flow is often overlooked.

The upscale eddy forcing from the high-frequency eddies to the low-frequency processes, which has been extensively discussed in previous studies, is confirmed here. However, we find that this eddy forcing works mainly in NAO−, and appears weak or even disappears in NAO+ if only the intraseasonal component is considered. This updates the knowledge about the role of the upscale energy transfer to low-frequency processes in previous studies, where this kind of forcing is believed independent of the low-frequency process phase.

Further analysis shows that the barotropic instability of the basic flow compensates for the lack of enough upscale eddy forcing in maintaining NAO+. Apart from the antisymmetric distribution of the kinetic energy transfer patterns, in between the northern cell and the southern cell over the Atlantic, for NAO+, there is a very strong canonical transfer from the basic flow window to the intraseasonal window, while for NAO−, there lies a dipolar pattern. These findings here show that the mechanisms underlying the intraseasonal NAO+ and NAO− are quite different: The barotropic instability of the basic flow dominates the development of the former, while the upscale forcing of the chaotic storms dominates that of the latter. This new finding, to our best knowledge, has never been documented in previous studies where only the role of upscale forcing from high-frequency storms to NAO is emphasized (e.g., Barnes & Hartmann, 2010; Luo et al., 2018; and Zhao et al., 2023).

Data Availability Statement

The ERA-40 datasets in this study are from https://apps.ecmwf.int/datasets/data/era40-daily/levtype=sfc/. The NAO index is obtained from https://ftp.cpc.ncep.noaa.gov/cwlinks/norm.daily.nao.cdas.z500.19500101_current.csv. Scripts of multiscale window transform and multiscale energy analysis are available on http://www.ncoads.org/article/show/67.aspx.

Acknowledgments
We are grateful to Suzana Camargo and two anonymous reviewers for their constructive suggestions. This study is partially supported by National Natural Science Foundation of China under Grants 42005052, 41975064, and 42230105, by Southern Marine Science and Engineering Guangdong Laboratory (Zhuhai) through the Startup Foundation, by Shanghai B & R Joint Laboratory Project (#22230750300), and by Shanghai International Science and Technology Partnership Project (#21230780200).

References

Baldwin, M. P., & Dunkerton, T. J. (1999). Propagation of the Arctic Oscillation from the stratosphere to the troposphere. *Journal of Geophysical Research*, *104*(D24), 30937–30946. https://doi.org/10.1029/1999JD900445

Baldwin, M. P., & Dunkerton, T. J. (2001). Stratospheric harbingers of anomalous weather regimes. *Science*, *294*(5542), 581–584. https://doi.org/10.1126/science.1063315

Barnes, E. A., & Hartmann, D. L. (2010). Dynamical feedbacks and the persistence of the NAO. *Journal of the Atmospheric Sciences*, *67*(3), 851–865. https://doi.org/10.1175/2009JAS3193.1

Barnes, E. A., Hartmann, D. L., Frierson, D. M. W., & Kidston, J. (2010). Effect of latitude on the persistence of eddy-driven jets. *Geophysical Research Letters*, *37*(11). https://doi.org/10.1029/2010GL043199

Barnston, A. G., & Livezey, R. E. (1987). Classification, seasonality and persistence of low-frequency atmospheric circulation patterns. *Monthly Weather Review*, *115*(6), 1083–1126. https://doi.org/10.1175/1520-0493(1987)115<1083:CSAPOL>2.0.CO;2

Cai, M., & Mak, M. (1990). Symbiotic relation between planetary and synoptic-scale waves. *Journal of the Atmospheric Sciences*, *47*(24), 2953–2968. https://doi.org/10.1175/1520-0469(1990)047<2953:SRBPAS>2.0.CO;2

Cohen, J., & Barlow, M. (2005). The NAO, the AO, and global warming: How closely related? *Journal of Climate*, *18*(21), 4498–4513. https://doi.org/10.1175/JCLI3530.1

DeWeaver, E., & Nigam, S. (2000a). Do stationary waves drive the zonal-mean jet anomalies of the northern winter? *Journal of Climate*, *13*(13), 2160–2176. https://doi.org/10.1175/1520-0442(2000)013<2160:DSWDTZ>2.0.CO;2

DeWeaver, E., & Nigam, S. (2000b). Zonal-eddy dynamics of the North Atlantic Oscillation. *Journal of Climate*, *13*(22), 3893–3914. https://doi.org/10.1175/1520-0442(2000)013<3893:ZEDOTN>2.0.CO;2

Feldstein, S., & Lee, S. (1998). Is the atmospheric zonal index driven by an eddy feedback? *Journal of the Atmospheric Sciences*, *55*(19), 3077–3086. https://doi.org/10.1175/1520-0469(1998)055<3077:ITAZID>2.0.CO;2

Feldstein, S. B. (2000). The timescale, power spectra, and climate noise properties of teleconnection patterns. *Journal of Climate*, *13*(24), 11–4440. https://doi.org/10.1175/1520-0442(2000)013<4430:ttpsac>2.0.co;2

Green, J. S. A. (1970). Transfer properties of the large-scale eddies and the general circulation of the atmosphere. *Quarterly Journal of the Royal Meteorological Society*, *96*(408), 157–185. https://doi.org/10.1002/qj.49709640802

Hansen, A. R., & Sutera, A. (1984). A comparison of the spectral energy and enstrophy budgets of blocking versus nonblocking periods. *Tellus A*, *36A*(1), 52–63. https://doi.org/10.1111/j.1600-0870.1984.tb00222.x

Hurrell, J. W. (1995). Decadal trends in the North Atlantic Oscillation: Regional temperatures and precipitation. *Science*, *269*(5224), 676–679. https://doi.org/10.1126/science.269.5224.676

Hurrell, J. W. (1996). Influence of variations in extratropical wintertime teleconnections on northern hemisphere temperature. *Geophysical Research Letters*, *23*(6), 665–668. https://doi.org/10.1029/96GL00459

Hurrell, J. W., Kushnir, Y., Ottersen, G., & Visbeck, M. (2003). An overview of the North Atlantic Oscillation. In *The North Atlantic Oscillation: Climatic significance and environmental impact* (pp. 1–35). American Geophysical Union (AGU). https://doi.org/10.1029/134GM01

Jin, F.-F. (2009). Eddy-induced instability for low-frequency variability. *Journal of the Atmospheric Sciences*, *67*(6), 1947–1964. https://doi.org/10.1175/2009JAS3185.1

Jin, F.-F., Pan, L.-L., & Watanabe, M. (2006). Dynamics of synoptic eddy and low-frequency flow interaction. Part II: A theory for low-frequency modes. *Journal of the Atmospheric Sciences*, *63*(7), 1695–1708. https://doi.org/10.1175/JAS3716.1

Kimoto, M., Jin, F.-F., Watanabe, M., & Yasutomi, N. (2001). Zonal—Eddy coupling and a neutral mode theory for the Arctic Oscillation. *Geophysical Research Letters*, *28*(4), 737–740. https://doi.org/10.1029/2000GL012377

Kug, J.-S., & Jin, F.-F. (2009). Left-hand rule for synoptic eddy feedback on low-frequency flow. *Geophysical Research Letters*, *36*(5), L05709. https://doi.org/10.1029/2008GL036435

Kushnir, Y. (1987). Retrograding wintertime low-frequency disturbances over the North Pacific Ocean. *Journal of the Atmospheric Sciences*, *44*(19), 2727–2742. https://doi.org/10.1175/1520-0469(1987)044<2727:RWLFDO>2.0.CO;2

Liang, X. S. (2016). Canonical transfer and multiscale energetics for primitive and quasigeostrophic atmospheres. *Journal of the Atmospheric Sciences*, *73*(11), 4439–4468. https://doi.org/10.1175/JAS-D-16-0131.1

Liang, X. S., & Anderson, D. (2007). Multiscale window transform. *Multiscale Modeling and Simulation*, *6*(2), 437–467. https://doi.org/10.1137/06066895X

Liang, X. S., & Robinson, A. R. (2005). Localized multiscale energy and vorticity analysis: I. Fundamentals. *Dynamics of Atmospheres and Oceans*, *38*(3), 195–230. https://doi.org/10.1016/j.dynatmoce.2004.12.004

Liang, X. S., & Robinson, A. R. (2007). Localized multi-scale energy and vorticity analysis: II. Finite-Amplitude instability theory and validation. *Dynamics of Atmospheres and Oceans*, *44*(2), 51–76. https://doi.org/10.1016/j.dynatmoce.2007.04.001

Limpasuvan, V., & Hartmann, D. L. (1999). Eddies and the annular modes of climate variability. *Geophysical Research Letters*, *26*(20), 3133–3136. https://doi.org/10.1029/1999GL010478

Lorenz, D. J., & Hartmann, D. L. (2001). Eddy–zonal flow feedback in the southern hemisphere. *Journal of the Atmospheric Sciences*, *58*(21), 3312–3327. https://doi.org/10.1175/1520-0469(2001)058<3312:EZFFIT>2.0.CO;2

Lorenz, E. N. (1955). Available potential energy and the maintenance of the general circulation. *Tellus*, *7*(2), 157–167. https://doi.org/10.1111/j.2153-3490.1955.tb01148.x

Luo, D. (2005). A barotropic envelope Rossby Soliton Model for block–eddy interaction. Part I: Effect of topography. *Journal of the Atmospheric Sciences*, *62*(1), 5–21. https://doi.org/10.1175/1186.1

Luo, D., Chen, X., & Feldstein, S. B. (2018). Linear and nonlinear dynamics of North Atlantic Oscillations: A new thinking of symmetry breaking. *Journal of the Atmospheric Sciences*, *75*(6), 1955–1977. https://doi.org/10.1175/JAS-D-17-0274.1

Luo, D., Gong, T., & Diao, Y. (2007). Dynamics of eddy-driven low-frequency dipole modes. Part III: Meridional displacement of westerly jet anomalies during two phases of NAO. *Journal of the Atmospheric Sciences*, *64*(9), 17–3248. https://doi.org/10.1175/jas3998.1

Luo, D., Zhong, L., & Franzke, C. L. E. (2015). Inverse energy cascades in an eddy-induced NAO-type flow: Scale interaction mechanism. *Journal of the Atmospheric Sciences*, *72*(9), 3417–3448. https://doi.org/10.1175/JAS-D-15-0062.1

Ma, J., & Liang, X. S. (2017). Multiscale dynamical processes underlying the wintertime Atlantic blockings. *Journal of the Atmospheric Sciences*, *74*(11), 3815–3831. https://doi.org/10.1175/JAS-D-16-0295.1

Oort, A. H. (1964). On estimates of the atmospheric energy cycle. *Monthly Weather Review*, *92*(11), 483–493. https://doi.org/10.1175/1520-0493(1964)092<0483:OEOTAE>2.3.CO;2

Plumb, R. A. (1983). A new look at the energy cycle. *Journal of the Atmospheric Sciences*, *40*(7), 1669–1688. https://doi.org/10.1175/1520-0469(1983)040<1669:ANLATE>2.0.CO;2

Ren, H.-L., Jin, F.-F., & Gao, L. (2012). Anatomy of synoptic eddy–NAO interaction through eddy structure decomposition. *Journal of the Atmospheric Sciences*, *69*(7), 2171–2191. https://doi.org/10.1175/JAS-D-11-069.1

Ren, H.-L., Jin, F.-F., Kug, J.-S., Zhao, J.-X., & Park, J. (2009). A kinematic mechanism for positive feedback between synoptic eddies and NAO. *Geophysical Research Letters*, *36*(11), L11709. https://doi.org/10.1029/2009GL037294

Ren, H.-L., Zhou, F., Nie, Y., & Zhao, S. (2022). Dynamic synoptic eddy feedbacks contributing to maintenance and propagation of intraseasonal NAO. *Geophysical Research Letters*, *49*(2), e2021GL096508. https://doi.org/10.1029/2021GL096508

Rennert, K. J., & Wallace, J. M. (2009). Cross-frequency coupling, skewness, and blocking in the northern hemisphere winter circulation. *Journal of Climate*, *22*(21), 5650–5666. https://doi.org/10.1175/2009JCLI2669.1

Robinson, W. A. (1991). The dynamics of low-frequency variability in a simple model of the global atmosphere. *Journal of the Atmospheric Sciences*, *48*(3), 429–441. https://doi.org/10.1175/1520-0469(1991)048<0429:TDOLFV>2.0.CO;2

Robinson, W. A. (1996). Does eddy feedback sustain variability in the zonal index? *Journal of the Atmospheric Sciences*, *53*(23), 3556–3569. https://doi.org/10.1175/1520-0469(1996)053<3556:DEFSVI>2.0.CO;2

Robinson, W. A. (2000). A baroclinic mechanism for the eddy feedback on the zonal index. *Journal of the Atmospheric Sciences*, *57*(3), 415–422. https://doi.org/10.1175/1520-0469(2000)057<0415:ABMFTE>2.0.CO;2

Robinson, W. A. (2006). On the self-maintenance of midlatitude jets. *Journal of the Atmospheric Sciences*, *63*(8), 2109–2122. https://doi.org/10.1175/JAS3732.1

Schmith, T., Olsen, S. M., Yang, S., & Christensen, J. H. (2022). Asymmetries in circulation anomalies related to the phases of the North Atlantic Oscillation on synoptic time scales. *Geophysical Research Letters*, *49*(11), e2022GL098149. https://doi.org/10.1029/2022GL098149

Shutts, G. J. (1983). The propagation of eddies in diffluent jetstreams: Eddy vorticity forcing of 'blocking' flow fields. *Quarterly Journal of the Royal Meteorological Society*, *109*(462), 737–761. https://doi.org/10.1002/qj.49710946204

Song, J. (2016). Understanding anomalous eddy vorticity forcing in North Atlantic Oscillation events. *Journal of the Atmospheric Sciences*, *73*(8), 2985–3007. https://doi.org/10.1175/JAS-D-15-0253.1

Thompson, D. W. J., & Wallace, J. M. (1998). The Arctic oscillation signature in the wintertime geopotential height and temperature fields. *Geophysical Research Letters*, *25*(9), 1297–1300. https://doi.org/10.1029/98GL00950

Uppala, S. M., KÅllberg, P. W., Simmons, A. J., Andrae, U., Bechtold, V. D. C., Fiorino, M., et al. (2005). The ERA-40 re-analysis. *Quarterly Journal of the Royal Meteorological Society*, *131*(612), 2961–3012. https://doi.org/10.1256/qj.04.176

Walker, G. T., & Bliss, E. W. (1932). *World weather V* (Vol. 4, pp. 53–84). Memoirs of the Royal Meteorological Society.

Xu, F., & Liang, X. S. (2020). The synchronization between the zonal jet stream and temperature anomalies leads to an extremely freezing North America in January 2019. *Geophysical Research Letters*, *47*(19), e2020GL089689. https://doi.org/10.1029/2020GL089689

Yang, Y., Weisberg, R. H., Liu, Y., & San Liang, X. (2020). Instabilities and multiscale interactions underlying the loop current eddy shedding in the Gulf of Mexico. *Journal of Physical Oceanography*, *50*(5), 1289–1317. https://doi.org/10.1175/JPO-D-19-0202.1

Zhang, Y., Yang, X.-Q., Nie, Y., & Chen, G. (2012). Annular mode–like variation in a multilayer quasigeostrophic model. *Journal of the Atmospheric Sciences*, *69*(10), 2940–2958. https://doi.org/10.1175/JAS-D-11-0214.1

Zhao, S., Ren, H.-L., Zhou, F., Scaife, A. A., & Nie, Y. (2023). Phase asymmetry in synoptic eddy feedbacks on the negatively-skewed winter NAO. *Atmospheric Research*, *288*, 106725. https://doi.org/10.1016/j.atmosres.2023.106725

Zhao, Y.-B., Liang, X. S., Guan, Z., & Hodges, K. I. (2019). The asymmetric eddy–background flow interaction in the North Pacific storm track. *Quarterly Journal of the Royal Meteorological Society*, *145*(719), 575–596. https://doi.org/10.1002/qj.3453